ANL/CSE-13/23

Radiolysis of Nitrate and Sulfate Solutions

Chemical Science and Engineering Division

About Argonne National Laboratory
Argonne is a U.S. Department of Energy laboratory managed by UChicago Argonne, LLC under contract DE-AC02-06CH11357. The Laboratory's main facility is outside Chicago, at 9700 South Cass Avenue, Argonne, Illinois 60439. For information about Argonne and its pioneering science and technology programs, see www.anl.gov.

DOCUMENT AVAILABILITY

Online Access: U.S. Department of Energy (DOE) reports produced after 1991 and a growing number of pre-1991 documents are available free via DOE's SciTech Connect (http://www.osti.gov/scitech/)

Reports not in digital format may be purchased by the public from the National Technical Information Service (NTIS):

U.S. Department of Commerce
National Technical Information Service
5301 Shawnee Rd
Alexandra, VA 22312
www.ntis.gov
Phone: (800) 553-NTIS (6847) or (703) 605-6000
Fax: (703) 605-6900
Email: **orders@ntis.gov**

Reports not in digital format are available to DOE and DOE contractors from the Office of Scientific and Technical Information (OSTI):

U.S. Department of Energy
Office of Scientific and Technical Information
P.O. Box 62
Oak Ridge, TN 37831-0062
www.osti.gov
Phone: (865) 576-8401
Fax: (865) 576-5728
Email: **reports@osti.gov**

Disclaimer
This report was prepared as an account of work sponsored by an agency of the United States Government. Neither the United States Government nor any agency thereof, nor UChicago Argonne, LLC, nor any of their employees or officers, makes any warranty, express or implied, or assumes any legal liability or responsibility for the accuracy, completeness, or usefulness of any information, apparatus, product, or process disclosed, or represents that its use would not infringe privately owned rights. Reference herein to any specific commercial product, process, or service by trade name, trademark, manufacturer, or otherwise, does not necessarily constitute or imply its endorsement, recommendation, or favoring by the United States Government or any agency thereof. The views and opinions of document authors expressed herein do not necessarily state or reflect those of the United States Government or any agency thereof, Argonne National Laboratory, or UChicago Argonne, LLC.

ANL/CSE-13/23

Radiolysis of Nitrate and Sulfate Solutions

---

by
Michael Kalensky, Sergey Chemerisov, Amanda Youker, Andrew Hebden, Peter Tkac,
Vakhtang Makarashvili, Elizabeth Krahn, John Krebs, Kevin Quigley, Robert Lowe, Delbert Bowers,
Seema Niak, Don Graczyk, Vivian Sullivan, Allen Bakel, and George F. Vandegrift
Chemical Science and Engineering Division, Argonne National Laboratory

prepared for
U.S. Department of Energy, National Nuclear Security Administration,
Office of Defense Nuclear Nonproliferation

November 20, 2012

CONTENTS

CONTENTS (CONT.)

FIGURES

FIGURES (CONT.)

TABLES

RADIOLYSIS OF NITRATE AND SULFATE SOLUTIONS

1 INTRODUCTION

Argonne National Laboratory (Argonne) is assisting two of the potential domestic producers, Babcock and Wilcox Technical Services Group (B&W) and Morgridge Institute for Research (MIR), in the development of a Mo-99 production pathway that do not use high enriched uranium (HEU), as part of the National Nuclear Security Administration (NNSA) Global Threat Reduction Initiative's (GTRI) program. B&W is developing the Medical Isotope Production System (MIPS); in this system, the Mo-99 is produced in a low enriched uranium (LEU)-fueled aqueous homogenous reactor (AHR) by the fission of U-235. MIR is developing the Subcritical Hybrid Intense Neutron Emitter (SHINE), which creates Mo-99 by neutron-induced fission of LEU in a sub-critical aqueous solution. One difference between the two is that MIR is considering aqueous uranyl-sulfate as the target solution, while B&W is planning to use aqueous uranyl nitrate as the fuel solution.

Experiments were performed at the Van de Graff accelerator facility to analyze the gases evolved as a result of low Linear Energy Transfer (LET) bombardment of various salt solutions. The experiments were designed to simulate the conditions inside the sub-critical solutions of the MIPS/SHINE Mo-99 production systems. During irradiation, radiolytic gases are generated from solution though decomposition of water and nitrate to form gaseous hydrogen, oxygen, and various compounds of nitrogen (nitrite-ammonia).

The purpose of this experiment was to determine the composition of radiolytically generated gases from nitrate and sulfate solutions. The solutions were chosen to simulate uranyl salt solutions that could possibly be used in a fuel or target solution for the generation of Mo-99. The electron beam will simulate the radiation field that will exist inside the reactor.

2 THEORY OF INTERACTIONS

Energy is deposited along tracks of the LET particles where the reactions involved in radiolysis occur. Several molecular, ionic, and radical species are produced in water.

$$e^{-}\,\mathrm{aq},\ \mathrm{OH}^{\cdot},\ \mathrm{H}^{\cdot},\ \mathrm{H_2O_2},\ \mathrm{H_2},\ \mathrm{H^+}$$

Some of the major reactions occurring are as follows.

$$\mathrm{H_2O} \rightarrow \mathrm{H_2O^+},\ e^{-},\ \mathrm{H_2O}$$

$$\mathrm{H_2O^+} + \mathrm{H_2O} \rightarrow \mathrm{H_3O^+} + \mathrm{OH}$$

$$\mathrm{H_2O}^{\cdot} \rightarrow \mathrm{H}\cdot + \mathrm{OH}$$

$$e^{-} \rightarrow e^{-}\,\mathrm{aq}$$

$$e^{-}\,\mathrm{aq} + \mathrm{H_2O} \rightarrow \mathrm{H}\cdot + \mathrm{OH^-}$$

$$e^{-}\,\mathrm{aq} + 2\mathrm{H}\cdot \rightarrow \mathrm{H_2}$$

$$e^{-}\,\mathrm{aq} + \mathrm{H_3O^+} \rightarrow \mathrm{H_2O} + \mathrm{H}$$

$$e^{-}\,\mathrm{aq} + \mathrm{OH}\cdot \rightarrow \mathrm{OH^-}$$

$$\mathrm{H} + \mathrm{OH}\cdot \rightarrow \mathrm{H_2O}$$

$$2\mathrm{OH}\cdot \rightarrow \mathrm{H_2O_2}$$

$$\mathrm{OH} + \mathrm{H_2O_2} \rightarrow \mathrm{HO_2} + \mathrm{H_2O}$$

$$2\mathrm{HO_2} \rightarrow \mathrm{H_2O_2} + \mathrm{O_2}$$

$$\mathrm{H_3O^+} + \mathrm{OH}\cdot \leftrightarrow 2\mathrm{H_2O}$$

When nitrate is in solution, its radiolysis has an even more complex set of possible reactions.

3 EXPERIMENTAL SETUP

The setup (see Figure 1) was designed with two interconnected systems, the process loop and the sampling manifold. The process loop is a closed loop of stainless steel tubing that consists of the target sample, the electron beam, and a peristaltic pump. The target sample is inserted into a holder directly in the accelerator beam path. The holder is attached to a recirculating pump and water bath to provide continuous cooling to the sample. The electron beam impinges on the cooling water and quartz tube in the setup. Mostly electrons and some X-rays interact with the test solution, and radiolytic gases are generated in the sample tube. The sample tube has an inlet and outlet through which headspace gases can be continuously recirculated throughout the process loop. Recirculation of gas is achieved using a peristaltic pump. The Van de Graff accelerator has a 3 MeV pulsed-electron beam.

The sampling manifold is connected to the process loop by a bellows valve. The sampling manifold consists of a capacitance monometer, a vacuum pump, and two analytical instruments connected by stainless steel tubing and a series of valves used to either evacuate, measure the pressure of, or analyze the gaseous constituents in the manifold. The gases are analyzed using two gas chromatographs (GCs). One GC (a SRI-8610C) has a thermal conductivity detector (TCD) and a helium ionization detector (HID). Separation is achieved with a molecular sieve and HayeSep-D columns. The other GC (a Shimadzu QP2010) has a TCD and a quadrapole mass selective detector (MS) with two molecular sieve 5A columns.

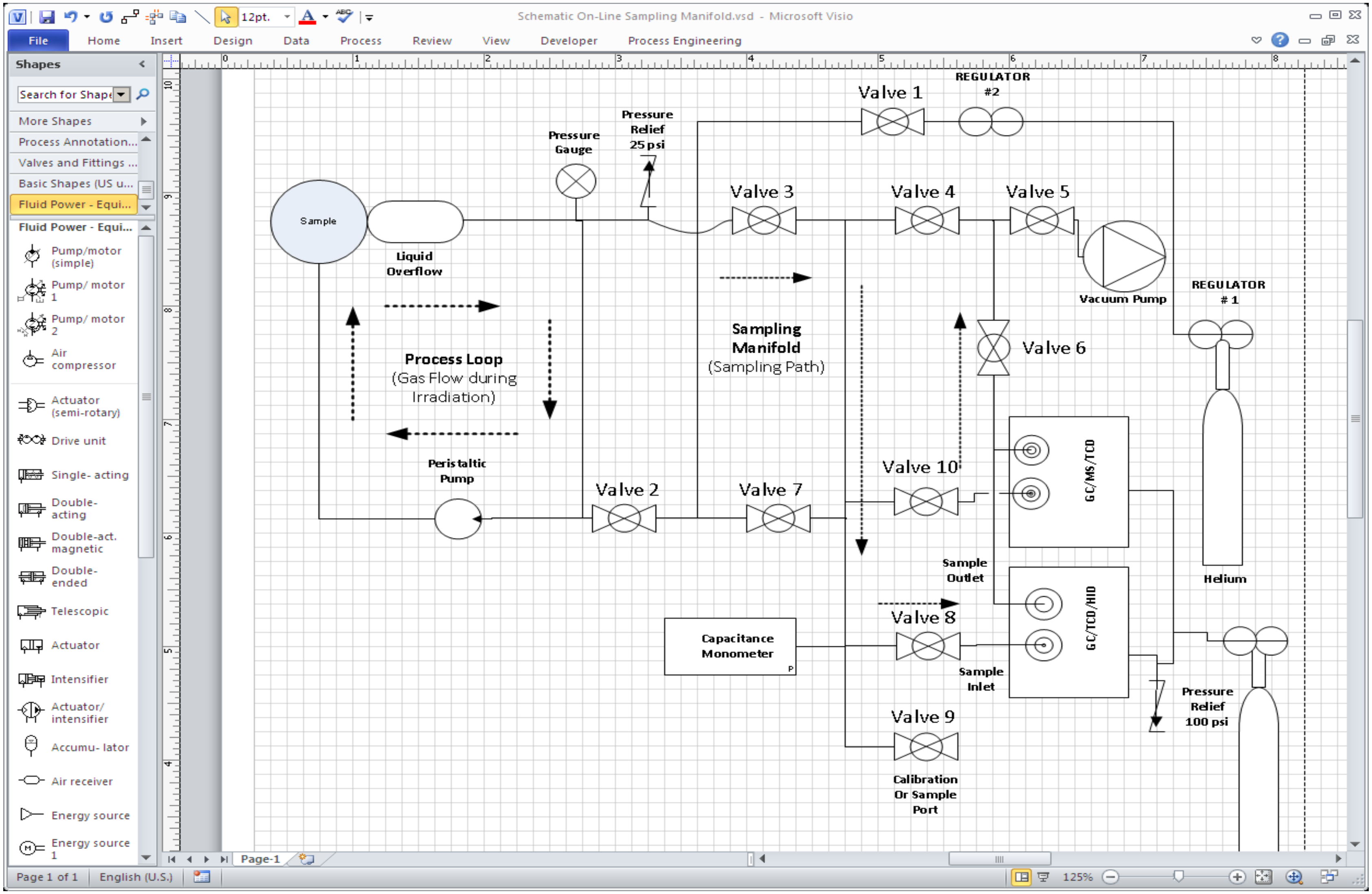

FIGURE 1 Experimental Setup

4 PROCEDURE

4.1 RADIOLYSIS STUDIES

A 2 ml test solution is placed into a quartz sample tube. The solution is purged with helium for several minutes to remove dissolved atmospheric gases (this process is not done with uranium solutions for safety concerns). The sample tube is connected to the process loop in the beam path. The system is then evacuated and purged with helium several times to remove atmospheric gases. The process loop is pressurized to 800 torr with ultrahigh purity (UHP) helium.

The 3 MeV electron beam is set to 20 µA power, and the sample is irradiated for approximately 5 hr. Periodically, at 30 min intervals, a sample of the headspace gas is withdrawn into the evacuated “sampling manifold” for analysis. The gas removed is replaced with helium to keep a constant pressure in the system. Prior to this experiment, oxalic acid dosimetry was performed to determine the dose deposited into the sample.

4.2 TEST SOLUTIONS

Aqueous solutions of sodium nitrate, sodium sulfate, uranyl nitrate, and uranyl sulfate at various concentrations and pH were irradiated.

- $NaNO_3$ was tested at four concentrations; 0.76 M, 1.26 M, 1.68 M, and 2.52 M. Each of these $NaNO_3$ concentrations was tested at three pH values, 0.70, 1.0, and 1.3.
- Na_2SO_4 was tested at concentrations of 0.46 M, 0.59 M, and 1.26 M at pH = 1 and at 0.38 M and 0.63 M at pH = 1.3.
- $UO_2(NO_3)_2$ was tested at 90, 150, 200, and 300 g-U/L, all at pH = 1.
- UO_2SO_4 was tested at 90 and 150g-U/L at pH = 1.

Also tested were RODI water, 0.1 M HNO_3, and 0.1 M H_2SO_4.

4.3 CORROSION STUDIES

The corrosion experiments were designed to simulate an aluminum vessel containing one of the solutions during irradiation. The purpose was to examine if an aluminum vessel could withstand the radiation and corroding effects of the sodium salt solutions. A coupon of aluminum (1100 grade) was placed inside the sample tube with one of the sodium nitrate or sulfate solutions. Then the sample was irradiated. Test solutions were 2.52 M $NaNO_3$ at pH = 1.3 and 0.63 M Na_2SO_4 at pH = 1.3.

5 GENERAL DISCUSSION OF THE DATA

No attempt was made to analyze the gases dissolved in solution. The solution was not continuously purged during irradiation to release dissolved gases. It was assumed that gases would dissolve in solution, react, or undergo radiolysis during the experiment. Each data point in the graphs represents the accumulated gases in the headspace of the system at sampling time.

Oxides of nitrogen N_2O and NO were detected during nitrate analysis but not reported as the total produced since the values fluctuated during irradiation. This is probably due to continuous reactions with water, oxygen, and solvated electrons. They can act as electron scavengers in solution forming N_2 and ammonia and may compete with hydrogen formation. Small amounts of nitrogen were detected and increased slightly throughout the test, but within the scope and design of this test, it could not be determined if the N_2 was being generated, entering through leaks, or from out-gassing of the system. A baseline "leak rate" was determined while no experiments were being run so that the nitrogen detected was either a leak or out-gassing from the stainless steel components. The amounts detected were comparable to those detected during the experiments. Therefore, the assumption was made that nitrogen was a contaminant and that detected was not from radiolysis. In the same test, small amounts of oxygen were detected as a contaminant. Thus the oxygen values reported are corrected by subtracting a value based on the amount of nitrogen detected related to the ratio of nitrogen to oxygen in air.

The solutions were analyzed for ammonium ion using ion chromatography. Analysis was performed using a Dionex IonPac CS12A analytical column equipped with a Dionex ED50 detector. Analysis occurred quite some time after the irradiation was performed. The samples were not preserved but were kept tightly closed. No appreciable amount of ammonium ion was detected in the solutions. Reporting limits were quite high since sodium and ammonium peaks were close in retention time; thus the high salt-concentration required dilution.

The results tables show final accumulated values at the end of the experiment. Hydrogen and oxygen values are reported as total µmoles produce during the entire run. Energy deposited in grays (Gy) is the accumulated dose. Values for "G" (molecules/100 eV) are reported as averaged over the entire experiment.

6 SODIUM NITRATE SOLUTIONS SUMMARY

Tables 1 through 5 and Figures 2 through 7 provide the experimental data for the irradiation of sodium nitrate solutions. The figures show total µmoles of analyte (either hydrogen or oxygen) versus accumulated dose (Gy) during the 5-hr experiment. Each data point is at sampling time for the analyte. Each figure contains results for the analyte at a particular sodium nitrate concentration and at a particular pH. The data in Table 1 are the final points on the corresponding figure. Figure 8 shows the H/O ratios for the data presented in Figures 2–7. The following is a summary of that data.

6.1 pH CHANGES

The first noteworthy result is the changes in pH after irradiation. Consistently, as the concentration of sodium nitrate increased, the pH increase became more dramatic. At low initial pH (pH = 0.7), the first concentrations (0.76 and 1.26 M) did not change, while 1.68 M rose by a ΔpH = 1.1, and the 2.52 M rose by a ΔpH = 4.9. The solution's initial pH had an effect on the amount of increase. At higher initial pH (pH = 1.3), the change from 0.76 M was slight (ΔpH = 0.05), but at 2.52 M, ΔpH was 8.75.

6.2 HYDROGEN AND OXYGEN EVOLUTION AND THE EFFECT OF SODIUM NITRATE CONCENTRATION

Two solutions at pH = 0.7 seem to lie outside the general trend of the data for 0.76 M and 1.26 M. It is not clear why they are outliers; reanalysis may be required to either confirm the result or drop the data as contaminated samples. Otherwise, all other solutions show a general trend of having an increase in H_2 and O_2 production with increasing salt concentration. The figures represent accumulated gas in the volume of headspace versus accumulated dose at each sampling time. Each data point represents a sample of gas taken during the experiment at 30-min intervals. Figures 2–7 follow with the tabular data but also show how hydrogen and oxygen concentrations increase over the course of the 5-hr experiment.

There was a clear increase in the production of H_2 and O_2 as the concentration of sodium nitrate was increased. This may seem to be counterintuitive since the energy deposited in solution could either act to follow a path in favor of H_2 and O_2 production or follow another path that does not. With any other molecular or ionic species in the water such sodium ions, there is an increasing probability that energy deposited in solution would be absorbed by those ions and not by a water molecule. Theoretically, the number of times a water molecule would follow the path to H_2 and O_2 production would decrease. It's not clear why this occurred and may not be within the scope of the tests performed. There was a slight increase in H_2 and O_2 production when nitrate in the form of nitric acid was added to the solution when compared to deionized water. This was not the case when comparing the sodium nitrate solutions across the different pH ranges. An increase in the H_3O^+ had little or no effect on the production of H_2 and O_2. This appears to be an effect of Na+ and/or NO_3^- concentration in the test solutions.

TABLE 1 Results of Sodium Nitrate Irradiations

Sample Concentration (M) $NaNO_3$	Energy Deposited (Gy)	Initial pH	Final pH	H_2 (µmoles)	O_2 (µmoles)	G Hydrogen (molecule/100 eV)	G Oxygen (molecule/100 eV)	H_2 to O_2 Ratio	NH_4 (mg/L)
0.76	2.25E+08	0.70	0.70	682	346	1.46E-02	7.40E-03	1.97	<20
1.26	2.30E+08	0.70	0.70	60	47	1.26E-03	9.83E-04	1.28	<40
1.68	2.27E+08	0.70	1.80	375	285	8.70E-03	6.61E-03	1.32	<50
2.52	2.35E+08	0.70	5.60	1767	1045	3.63E-02	2.14E-02	1.69	<60
0.76	2.36E+08	1.02	1.09	302	144	6.19E-03	2.94E-03	2.10	84.9
1.22	2.38E+08	1.00	1.38	607	332	1.23E-02	6.73E-03	1.83	<30
1.68	2.39E+08	1.01	2.06	530	292	1.07E-02	5.90E-03	1.81	<40
2.52	2.38E+08	1.01	8.75	2099	2275	4.26E-02	4.61E-02	0.92	<80
0.76	2.39E+08	1.30	1.35	278	125	5.61E-03	2.52E-03	2.23	<30
1.26	2.20E+08	1.30	1.40	288	151	6.33E-03	3.32E-03	1.91	100
1.68	2.30E+08	1.31	6.05	846	448	1.77E-02	9.39E-03	1.89	<50
2.52	2.29E+08	1.30	10.1	1865	1549	3.93E-02	3.27E-02	1.20	<60
0.1M HNO_3	2.56E+08	1.00	1.04	220	97	4.47E-03	1.96E-03	2.28	N.A.
RODI Water	2.35E+08	6.3	8.52	131	55	2.66E-03	1.12E-03	2.37	N.A.
(2.52 M@pH 1.3) Al Corrosion	2.26E+08	1.30	11.4	2396	2464	4.86E-02	5.00E-02	0.97	<60

TABLE 2 Initial pH = 0.7: N_2O and NO Values Are µmoles at Sampling Time

Sampling Time (min)	0.76 M $NaNO_3$		1.26 M $NaNO_3$		1.68 M $NaNO_3$		2.52 M $NaNO_3$	
	N_2O	NO	N_2O	NO	N_2O	NO	N_2O	NO
30	<0.05	<0.05	<0.05	<0.05	<0.05	<0.05	1.56	0.136
60	<0.05	<0.05	<0.05	<0.05	2.53	<0.05	7.53	0.491
90	<0.05	<0.05	<0.05	<0.05	2.53	<0.05	7.53	0.657
120	<0.05	<0.05	<0.05	<0.05	3.84	0.272	7.88	0.678
150	<0.05	<0.05	<0.05	<0.05	4.93	0.419	8.26	0.574
180	<0.05	<0.05	<0.05	<0.05	5.62	0.450	8.86	0.459
210	<0.05	<0.05	<0.05	0.491	6.63	0.555	9.05	0.386
240	<0.05	<0.05	0.063	0.480	6.57	0.534	8.81	0.313
270	0.208	<0.05	0.052	0.793	6.79	0.544	8.86	0.271
300	<0.05	0.073	N.A.	N.A.	6.79	0.544	8.96	0.230

TABLE 3 Initial pH = 1.0: N_2O and NO Values Are µmoles at Sampling Time

Sampling Time (min)	0.76 M $NaNO_3$		1.26 M $NaNO_3$		1.68 M $NaNO_3$		2.52 M $NaNO_3$	
	N_2O	NO	N_2O	NO	N_2O	NO	N_2O	NO
30	<0.5	<0.5	0.961	N.A.	<0.5	N.A.	<0.5	N.A.
60	<0.5	<0.5	2.47	N.A.	3.87	N.A.	5.34	N.A.
90	<0.5	<0.5	2.47	N.A.	3.87	N.A.	5.34	N.A.
120	<0.5	<0.5	2.88	N.A.	1.47	N.A.	5.55	N.A.
150	<0.5	<0.5	3.51	N.A.	4.82	N.A.	7.02	N.A.
180	<0.5	<0.5	1.90	N.A.	4.71	N.A.	8.90	N.A.
210	<0.5	<0.5	3.61	N.A.	5.13	N.A.	4.40	N.A.
240	<0.5	<0.5	3.77	N.A.	1.47	N.A.	6.60	N.A.
270	<0.5	<0.5	3.94	N.A.	4.61	N.A.	10.2	N.A.
300	<0.5	<0.5	3.61	N.A.	3.04	N.A.	10.8	N.A.

TABLE 4 Initial pH = 1.3: N_2O and NO Values Are µmoles at Sampling Time

Sampling Time (min)	0.76 M $NaNO_3$		1.26 M $NaNO_3$		1.68 M $NaNO_3$		2.52 M $NaNO_3$	
	N_2O	NO	N_2O	NO	N_2O	NO	N_2O	NO
30	<0.5	<0.5	<0.5	N.A.	<0.5	N.A.	1.54	<0.05
60	<0.5	<0.5	<0.5	N.A.	<0.5	N.A.	2.63	<0.05
90	<0.5	<0.5	<0.5	N.A.	<0.5	N.A.	2.63	<0.05
120	<0.5	<0.5	<0.5	N.A.	0.524	N.A.	2.93	<0.05
150	<0.5	<0.5	<0.5	N.A.	0.733	N.A.	3.15	<0.05
180	<0.5	<0.5	<0.5	N.A.	0.733	N.A.	3.08	0.104
210	<0.5	<0.5	<0.5	N.A.	1.68	N.A.	2.73	0.052
240	<0.5	<0.5	0.691	N.A.	1.15	N.A.	3.20	0.157
270	<0.5	<0.5	0.785	N.A.	1.68	N.A.	3.07	<0.05
300	<0.5	<0.5	0.754	N.A.	2.51	N.A.	N.A.	N.A.

TABLE 5 Initial pH = 1.3: N_2O and NO Values Are µmoles at Sampling Time

Sampling Time (min)	RODI Water		0.1 M HNO_3		Corr-2.52 M, pH 1.3	
	N_2O	NO	N_2O	NO	N_2O	NO
30	<0.05	<0.05	<0.05	<0.05	1.00	<0.05
60	<0.05	<0.05	<0.05	<0.05	1.71	0.136
90	<0.05	<0.05	<0.05	<0.05	1.71	0.126
120	<0.05	<0.05	<0.05	<0.05	2.03	0.115
150	<0.05	<0.05	<0.05	<0.05	2.35	0.094
180	<0.05	<0.05	<0.05	<0.05	2.78	0.073
210	<0.05	<0.05	<0.05	<0.05	2.80	0.052
240	<0.05	<0.05	<0.05	<0.05	3.02	<0.05
270	<0.05	<0.05	<0.05	<0.05	3.98	<0.05
300	<0.05	<0.05	<0.05	<0.05	5.36	<0.05

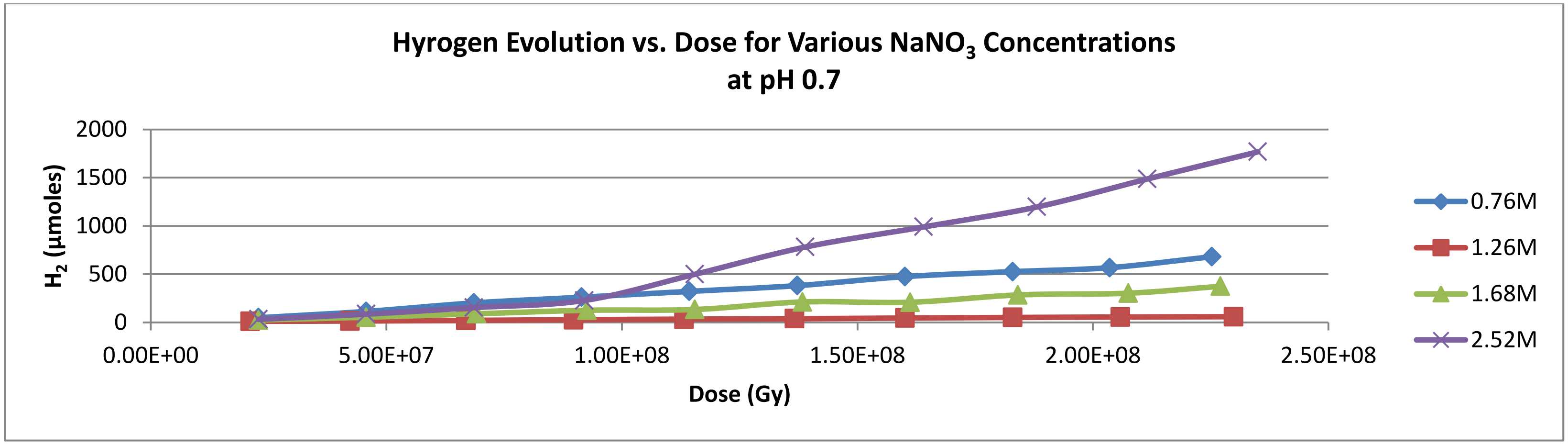

FIGURE 2 Hydrogen Production from $NaNO_3$ Solutions at pH = 0.7

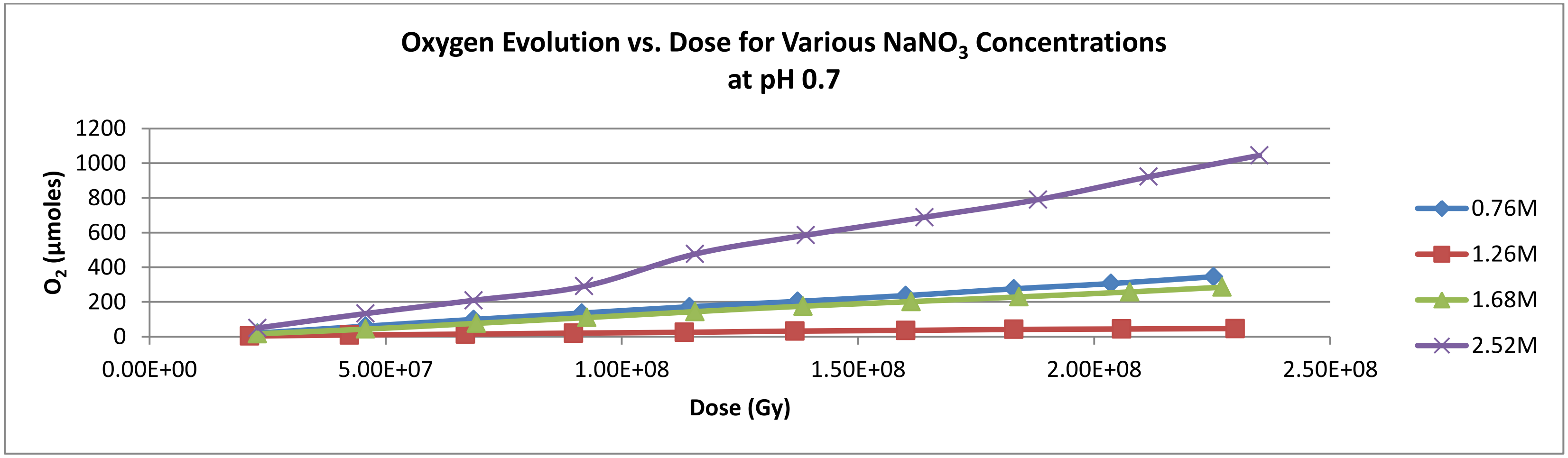

FIGURE 3 Oxygen Production from $NaNO_3$ Solutions at pH = 0.7

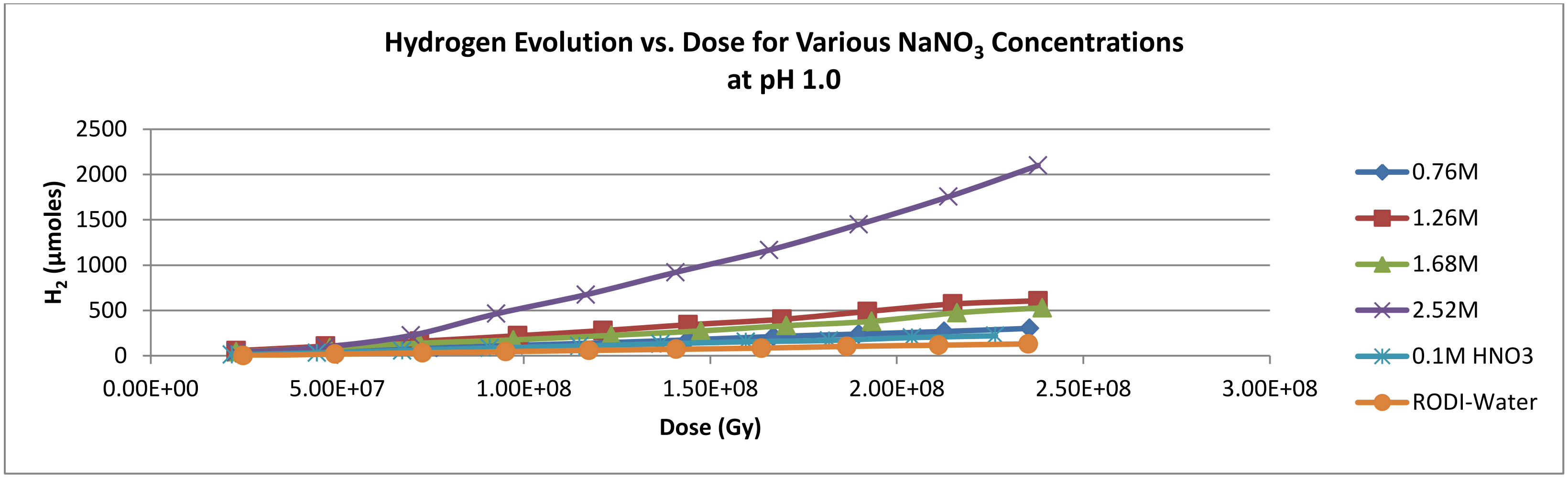

FIGURE 4 Hydrogen Production from NaNO$_3$ Solutions at pH = 1.0

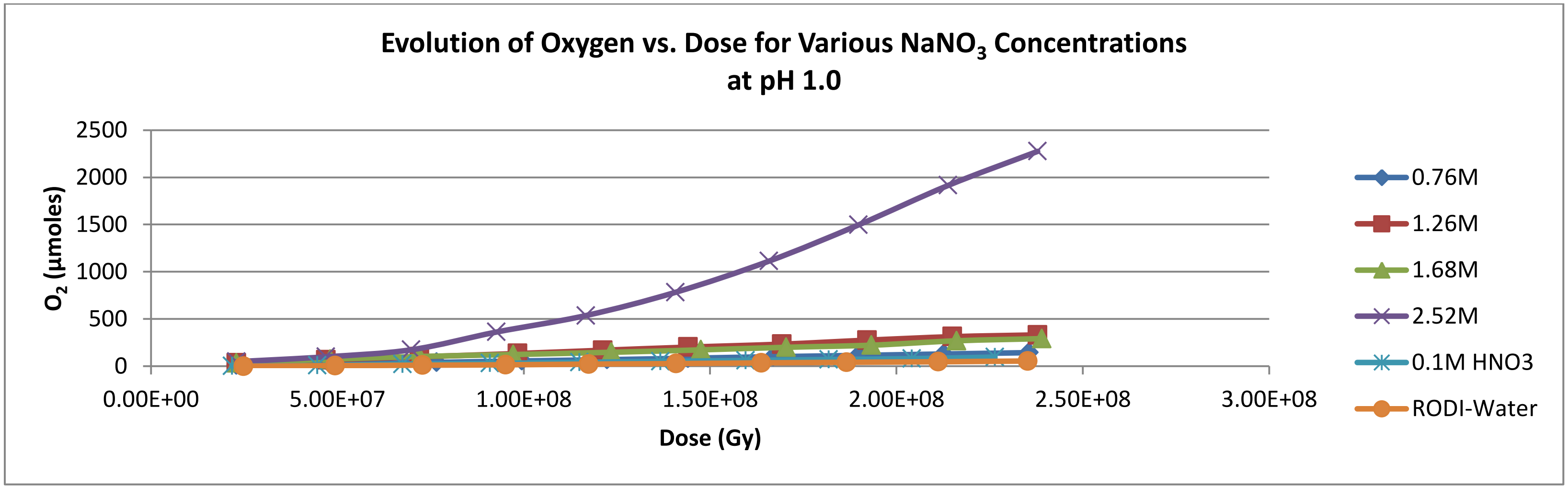

FIGURE 5 Oxygen Production from NaNO$_3$ Solutions at pH = 1.0

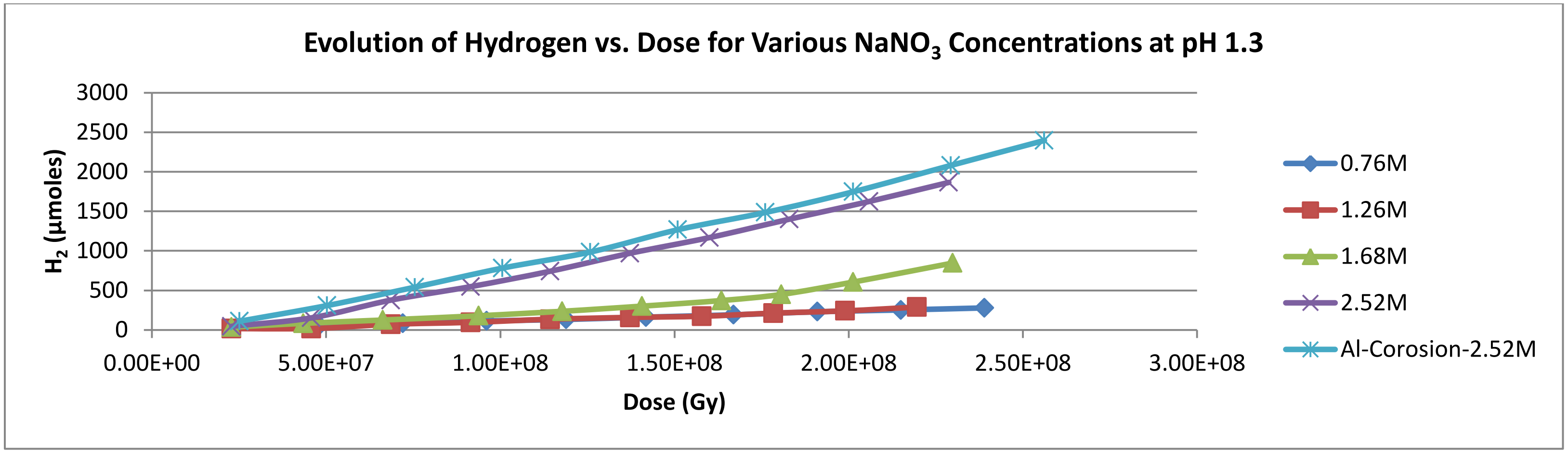

FIGURE 6 Hydrogen Production from $NaNO_3$ Solutions at pH = 1.3

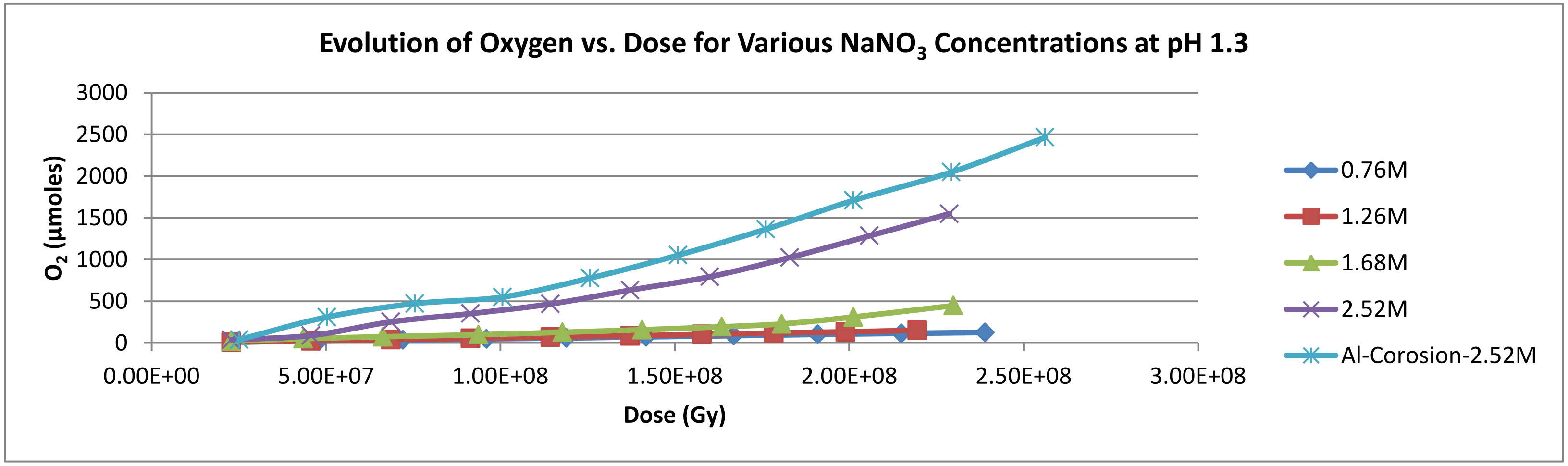

FIGURE 7 Oxygen Production from $NaNO_3$ Solutions at pH = 1.3

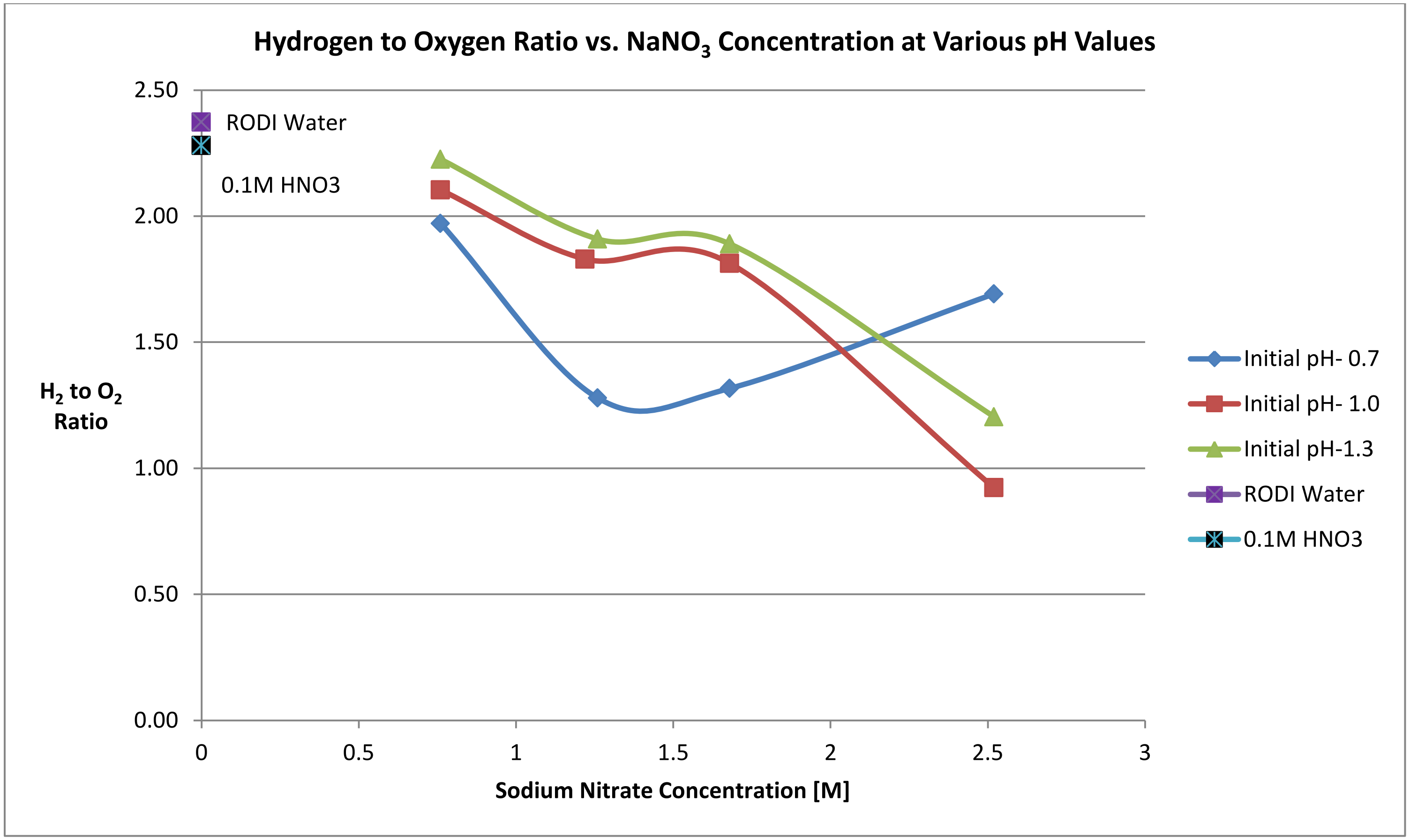

FIGURE 8 **Hydrogen to Oxygen Ratio vs. NaNO$_3$ Concentration at Various pH**

The sodium nitrate concentration also appeared to affect the ratio of hydrogen to oxygen. The H_2 to O_2 ratio decreased as the sodium nitrate concentration increased. This was exhibited across the different pH ranges. An increase in the sodium nitrate concentration increased the production of molecular oxygen relative to hydrogen. At low sodium nitrate concentration, deionized water and 0.1 M HNO_3, the ratio of H_2 to O_2 was near or above 2:1, but as the sodium nitrate concentration increased, that ratio decreased to near and below a value of 1:1.

6.3 CORROSION STUDY

The test for corrosion of aluminum in solution was performed using the 2.52 M sodium nitrate at pH = 1.3. This experiment was intended to simulate an aluminum vessel containing the solution during irradiation. After irradiation, the aluminum was weighed and found to have decreased in mass by 0.5 mg. A visible oxide layer was seen in the surface of the metal. The pH of the solution was found to have increased from 1.3 to 11.4. This result was similar to the solution without the aluminum coupon, which also showed a sharp increase in pH.

Hydrogen and oxygen production was similar to the test solution although slightly higher. Oxygen production was much higher. This was highlighted by the H_2 to O_2 ratio of 0.97:1 as compared to the solutions (1.20:1). One can assume that some of the energy was absorbed by the aluminum coupon instead of being deposited into the solution.

6.4 NITROUS OXIDE AND NITRIC OXIDE EVOLUTION

Tables 2, 3, 4, and 5 shows the evolution of N_2O and NO during the irradiation experiments. N.A. indicates that the analyte was not analyzed during that experiment. The tables indicate the total µmoles detected at sampling time (*t*). These data are displayed in this way for two reasons.

- The concentrations of analyte are below the lowest calibration standard though the peaks are detected.
- These compounds tend to be a very reactive species. NO reacts with oxygen to become NO_2, a very corrosive gas. It also can react in the presence of oxygen and water to form nitrous acid HNO_2.

When considering these factors, it was best to report the data as total umoles detected at time (*t*) instead of total accumulated µmoles.

7 SODIUM SULFATE SOLUTIONS SUMMARY

Table 6 and Figures 9 through 13 provide experimental data for the irradiation of sodium sulfate solutions. Figures 9 through 12 show total µmoles of analyte (either hydrogen or oxygen) versus accumulated dose (Gy) during the 5-hr experiment. Each data point is at the sampling time for the analyte. Each figure is displayed for the analyte at the various sodium sulfate concentrations at a particular pH. These data follow with the tabular data such that the final point on the graph is the value listed in Table 6. Figure 13 shows the H/O ratios for the data presented in Figures 9–12. The following is a summary of that data.

7.1 PH CHANGES

There were no significant changes in pH during the irradiation of sodium sulfate solution. This was seen across the various concentrations. The only pH change observed was in the aluminum corrosion study where the pH increased.

7.2 HYDROGEN AND OXYGEN EVOLUTION AND THE EFFECT OF SODIUM CONCENTRATION

The total production of hydrogen and oxygen was fairly consistent among the various low sodium sulfate concentrations. There may not have been enough variability in the salt to observe a change, since the highest (1.26 M Na_2SO_4) showed an increase in the totals produced. This probably follows with the nitrate solution such that increasing the sodium concentration will cause an increase in H_2 and O_2 production.

The hydrogen-to-oxygen ratio was consistent over the range of sodium sulfate concentrations. The ratio stays slightly above a ratio of 2 to 1. The buildup of hydrogen peroxide in solution along with the greater solubility of oxygen (7.6 mg/L at 20°C) as opposed to hydrogen (1.6 mg/L at 20°C) in water will tend to make the headspace gases richer in hydrogen. Deviations from a ratio of 2.2 to 1 across the range of concentrations were slight.

7.3 CORROSION STUDY

The test for corrosion of aluminum in solution was performed using the 0.63 M sodium sulfate at pH 1.3. This experiment was intended to simulate an aluminum vessel containing the solution during irradiation. After irradiation, the aluminum was weighed and found to have decreased in mass by 4.9 mg. The aluminum coupon retained its luster. The pH of the solution was found to have increased from pH 1.3 to 2.2. Hydrogen and oxygen production were markedly lower compared to the results with the same solution without the aluminum. This is probably partially due to the physical presence of the aluminum coupon absorbing some of the energy instead of being deposited in the solution. One striking difference was the decrease in oxygen highlighted by the H_2 to O_2 ratio of 5.77 to 1.

TABLE 6 Results from the Irradiation of Sodium Sulfate Solutions

$[Na_2SO_4]$ [M]	Energy Deposited (Gy)	pH		µmoles H_2 Total Produced	µmoles O_2 Total Produced	G-Value H_2 (molecules/100 eV)	G-Value O_2 (Molecules/100 eV)	H_2 to O_2 Ratio
		Initial	Final					
0.46	2.38E+08	1.01	0.95	652	291	1.37E-02	6.11E-03	2.24
0.59	2.36E+08	1.00	1.15	646	281	1.32E-02	5.76E-03	2.29
1.26	2.30E+08	1.01	1.01	1,092	508	2.29E-02	1.07E-02	2.15
0.38	2.24E+08	1.31	1.25	804	380	1.74E-02	8.20E-03	2.12
0.63	2.32E+08	1.31	1.15	610	267	1.27E-02	5.56E-03	2.28
RODI Water	2.35E+08	6.30	8.52	131	55	2.65E-03	1.12E-03	2.37
0.1 M H_2SO_4	2.23E+08	0.99	0.93	815	351	1.76E-02	7.59E-03	2.32
[0.63 M] Al Corrosion	2.44E+08	1.31	2.15	297	52	5.89E-03	1.02E-03	5.77

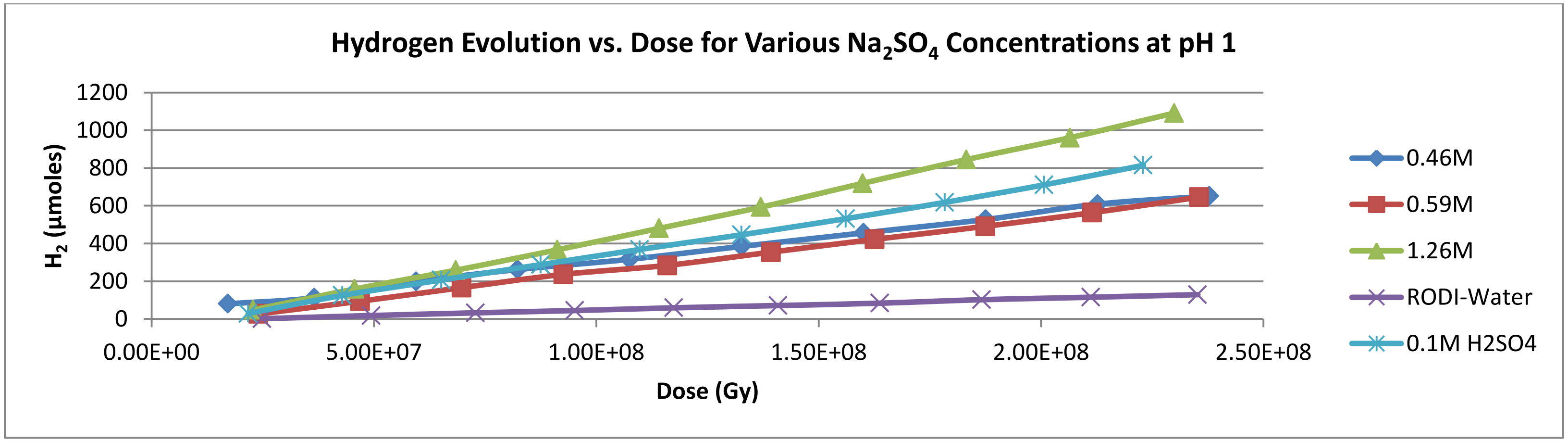

FIGURE 9 Hydrogen Production from Na_2SO_4 Solutions at pH = 1

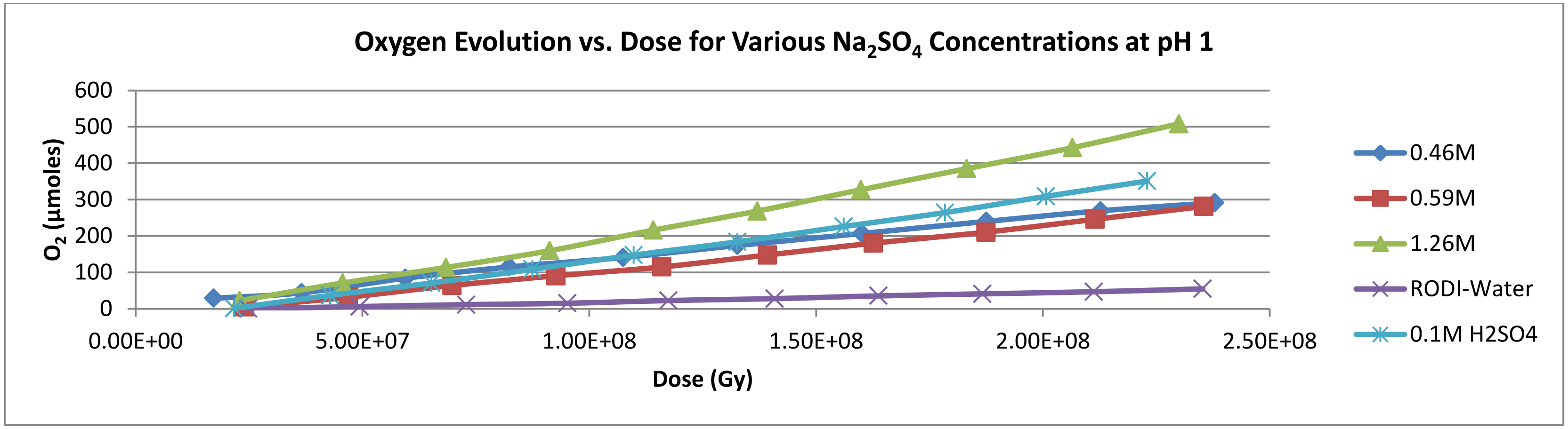

FIGURE 10 **Oxygen Production from Na_2SO_4 Solutions at pH = 1**

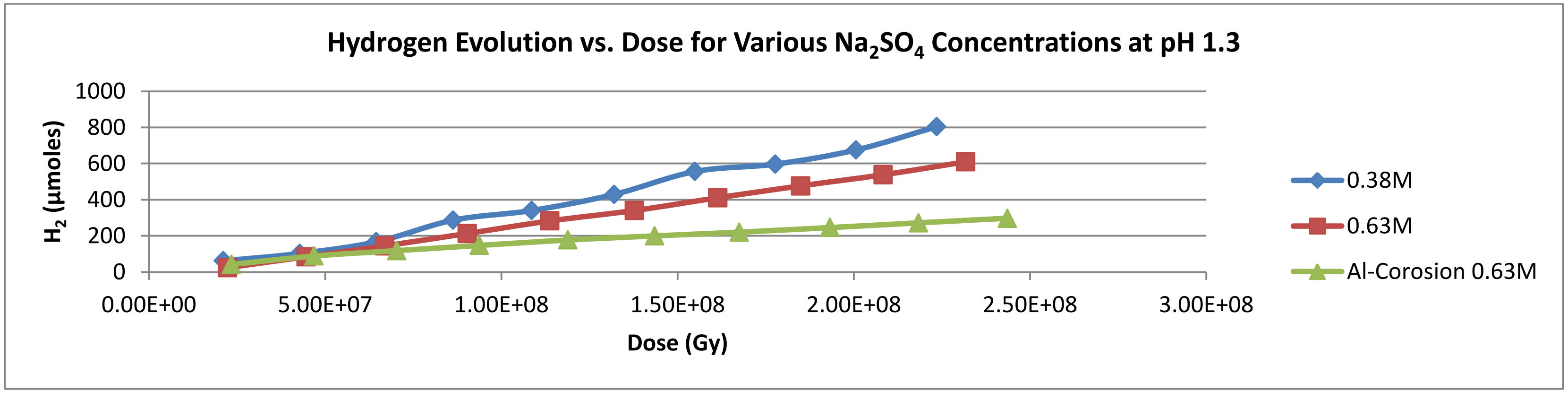

FIGURE 11 **Hydrogen Evolution from Na_2SO_4 Solutions at pH = 1.3**

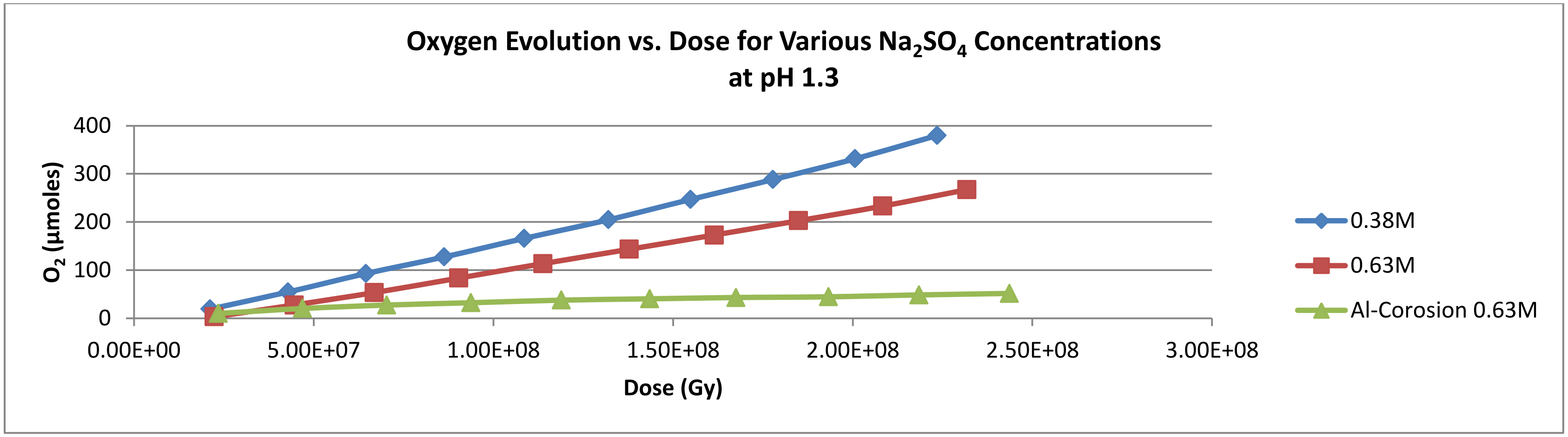

FIGURE 12 Oxygen Evolution from Na_2SO_4 Solutions at pH = 1.3

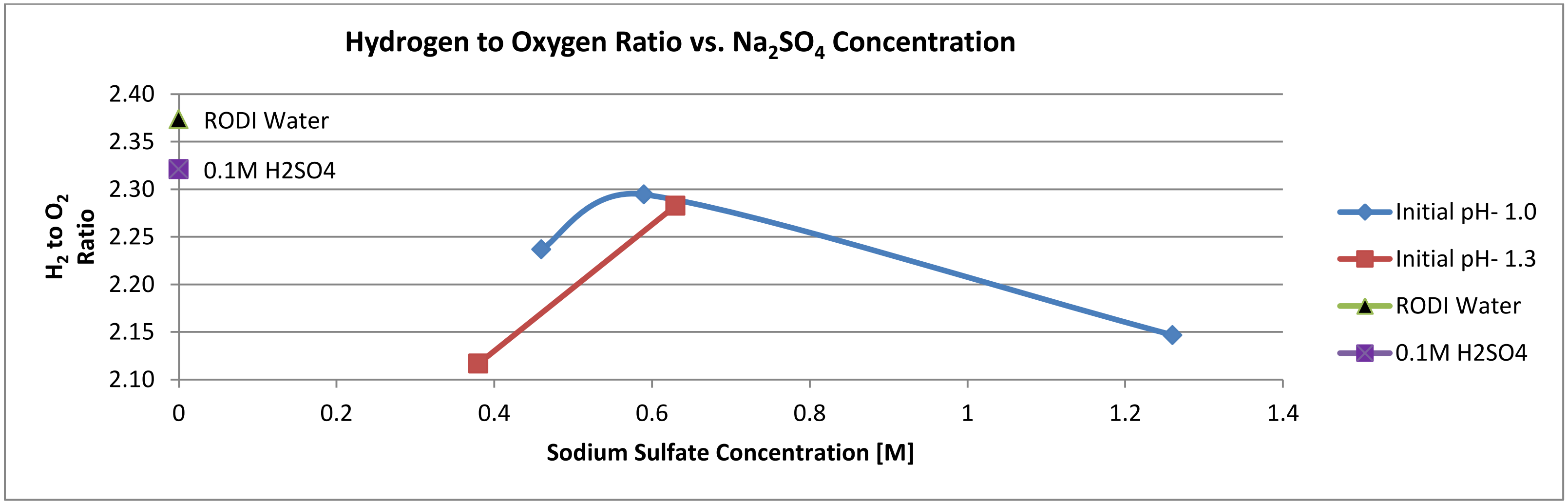

FIGURE 13 Hydrogen to Oxygen Ratio versus Na_2SO_4 Concentration at Various pH

8 URANYL NITRATE SOLUTIONS SUMMARY

Tables 7 and 8, and Figures 14 and 15, provide experimental data for the irradiation of uranyl nitrate solutions. The figures show total µmoles of analyte (either hydrogen or oxygen) versus accumulated dose (Gy) during the 5-hr experiment. Each data point is at the sampling time for the analyte. Each graph is displayed for the analyte at the various uranyl nitrate concentrations. These data follow with the tabular data such that the final point on the graph is the value listed in Table 7. The H/O ratios are presented in Figure 16. The following is a summary of that data.

8.1 pH CHANGES

There was a slight increase in pH during the irradiation of uranyl nitrate solutions. This was seen at the higher concentrations. The sample with the lowest uranyl concentration showed no observable pH change.

8.2 HYDROGEN AND OXYGEN EVOLUTION AND THE EFFECT OF SODIUM CONCENTRATION

The total production of hydrogen and oxygen was fairly consistent among the three high concentrations of uranyl nitrate. It is not until the lowest concentration is examined that a sharp increase in the total production of hydrogen and oxygen is observed. This is following the patterns of pH changes and H_2 to O_2 ratio versus the uranyl nitrate concentration. At the lowest concentration (76 g-U/L), the ratio is observed to be (1.75:1) as opposed to the highest (226 g-U/L) being at (1.17:1). Thus, the higher the uranyl nitrate concentration, the lower the total amount of hydrogen and oxygen will be produced, and the H_2/O_2 ratio will decrease.

8.3 NITROUS AND NITRIC OXIDE EVOLUTION

Table 8 shows the evolution of N_2O and NO during the irradiation of uranyl nitrate. N.A. indicates that the analyte was not analyzed during that experiment. The table indicates the µmoles detected at sampling time (*t*). These data are displayed in this fashion for several reasons. The concentrations of analyte are below the lowest calibration standard, although the peaks are detected. Also, the compounds tend to be very reactive species. NO reacts with oxygen to become NO_2. It also can react in the presence of oxygen and water to form nitrous acid HNO_2. When considering these factors, it was best to report the data as total µmoles detected at time (*t*) instead of total accumulated µmoles.

As the concentration of uranyl nitrate was increased, the production of the nitrous oxide increased. There was a lag between the start of the experiment and the first detection of this species. This was probably due to its solubility in solution.

TABLE 7 Data from the Irradiation of Uranyl Nitrate Solutions

Initial $UO_2(NO_3)_2$ [g-U/L]	Energy Deposited (Gy)	Final $UO_2(NO_3)_2$ [g-U/L]	pH Initial	pH Final	µmoles H_2 Total Produced	µmoles O_2 Total Produced	G-Value H_2 H_2/100 eV	G-Value O_2 O_2/100 eV	H_2 to O_2 Ratio
76	2.32E+08	No Precipitation	1.0	1.02	1241	708	2.49E-02	1.51E-02	1.75
128	2.33E+08	No Precipitation	1.0	1.84	692	489	1.43E-02	1.01E-02	1.41
175	2.32E+08	No Precipitation	1.0	2.21	645	519	1.34E-02	1.08E-02	1.24
226	2.05E+08	No Precipitation	1.0	2.09	645	550	1.51E-02	1.29E-02	1.17

TABLE 8 N_2O and NO in µmoles at Sampling Time for Irradiated Uranyl Nitrate Solutions

Sampling Time (min)	76 g-U/L N_2O	76 g-U/L NO	128 g-U/L N_2O	128 g-U/L NO	175 g-U/L N_2O	175 g-U/L NO	226 g-U/L N_2O	226 g-U/L NO
30	<0.5	<0.5	<0.5	<0.5	<0.5	<0.5	<0.5	<0.5
60	<0.5	<0.5	<0.5	<0.5	<0.5	<0.5	<0.5	<0.5
90	<0.5	<0.5	<0.5	<0.5	<0.5	<0.5	<0.5	<0.5
120	<0.5	<0.5	<0.5	<0.5	<0.5	<0.5	1.52	<0.5
150	<0.5	<0.5	<0.5	<0.5	<0.5	<0.5	3.05	<0.5
180	<0.5	<0.5	<0.5	<0.5	<0.5	<0.5	3.96	<0.5
210	<0.5	<0.5	<0.5	<0.5	1.32	<0.5	4.17	<0.5
240	<0.5	<0.5	<0.5	<0.5	2.84	<0.5	2.64	<0.5
270	<0.5	<0.5	<0.5	<0.5	2.24	<0.5	3.35	<0.5
300	<0.5	<0.5	<0.5	<0.5	2.03	<0.5	N.A.	N.A.

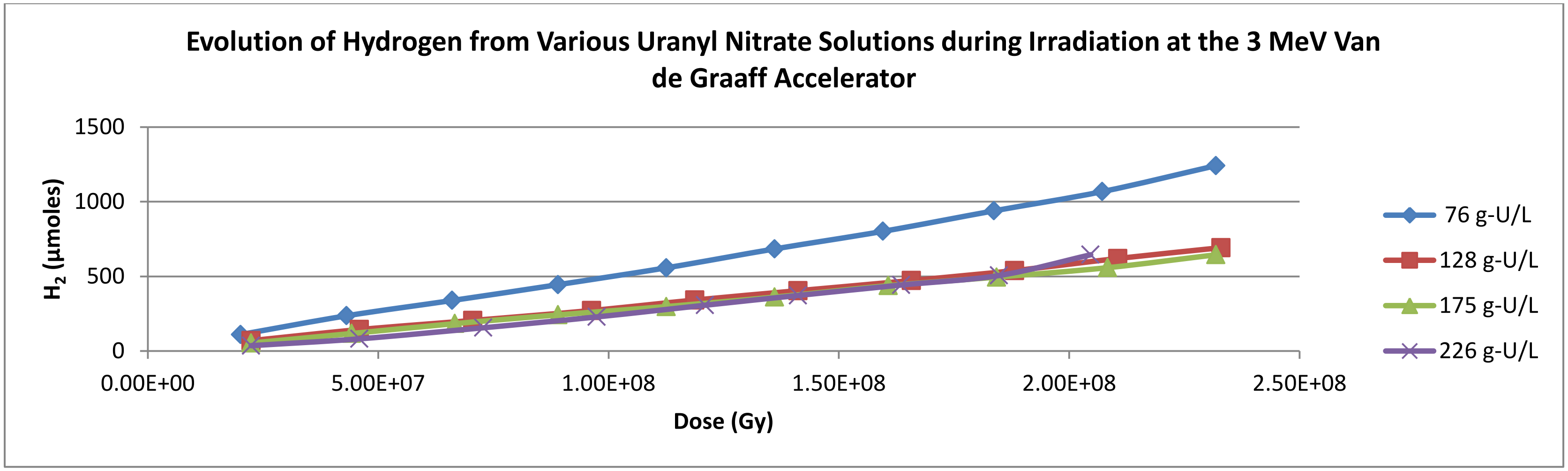

FIGURE 14 Hydrogen Evolution from $UO_2(NO_3)_2$ Solutions

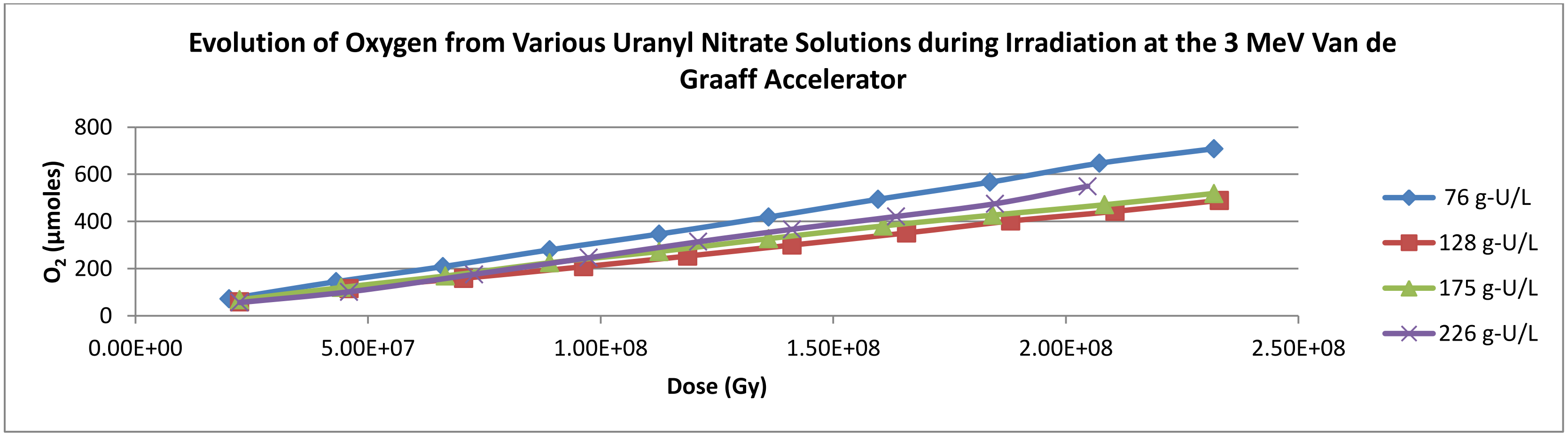

FIGURE 15 Oxygen Evolution from $UO_2(NO_3)_2$ Solutions

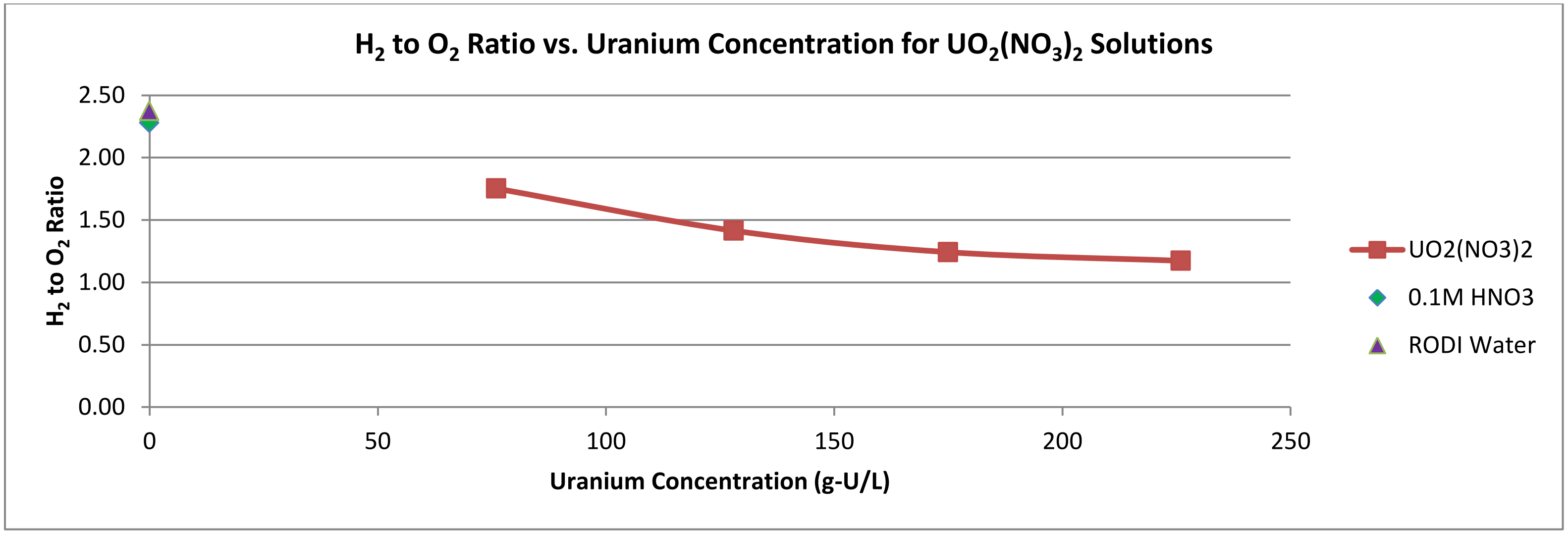

FIGURE 16 Oxygen Evolution from $UO_2(NO_3)_2$ Solutions

9 URANYL SULFATE SOLUTIONS SUMMARY

Table 9 and Figures 17 and 18 provide experimental data for the irradiation of uranyl sulfate solutions. Figures 17 and 18 show total µmoles of analyte (either hydrogen or oxygen) versus accumulated dose (Gy) during the 5-hr experiment. Each data point is at the sampling time for the analyte. Each graph is displayed for the analyte at the various uranyl sulfate concentrations at a particular pH. These data follow with the tabular data such that the final point on the graph is the value listed in Table 9. Figure 19 presents the H/O ratios for the data. The following is a summary of that data.

9.1 PRECIPITATION OF URANYL PEROXIDE

Uranyl peroxide was precipitated from solution for each of the uranyl sulfate experiments. It was assumed to be the peroxide because of previous experiments on uranyl sulfate solutions. The peroxide was also indicated by the fact that the solid redissolved when the slurry was in a hot water bath. Density measurements were performed on the post-irradiated solutions after the precipitate was filtered to determine the final resulting uranyl sulfate concentration. Those data are listed in Table 9. The percentage of uranium to precipitate decreased as the concentration of uranium increased. At 88 g-U/L, 28% or 24.5 g-U/L precipitated to a final concentration of 63.5 g-U/L. At 138 g-U/L, 16% or 22 g-U/L precipitated to a final concentration of 116 g-U/L. Finally at 298 g-U/L, 12% or 36 g-U/L precipitated to a final concentration of 262 g-U/L. Hydrogen peroxide formation during irradiation is assumed to be causing the precipitation. Experiments performed and listed in the next section show that this can be avoided by using a catalyst for peroxide destruction.

9.2 PH CHANGES

Consistently, the pH of all solutions decreased with dose. This was probably due to the formation of uranyl peroxide, which follows the equation $UO_2^{+2} + H_2O_2 + 2H_2O \leftrightarrow UO_2O_2 \cdot 2H_2O + 2H^+$.

9.3 HYDROGEN AND OXYGEN EVOLUTION

The production of hydrogen and oxygen was quite high for all experiments. There was a definite trend showing that as the uranyl sulfate concentration increased, the production of H_2 and O_2 decreased. The ratio of H_2:O_2 was at or slightly above 2:1, favoring the production of hydrogen as the uranium concentration was increased.

TABLE 9 Data from the Irradiation of Uranyl Sulfate Solutions

$[UO_2(SO_4)]$ [g-U/L]	Energy Deposited (Gy)	Final $[UO_2(SO_4)]$ [g-U/L]	pH		µmoles H_2 Total Produced	µmoles O_2 Total Produced	G-Value H_2 H_2/100 eV	G-Value O_2 O_2/100 eV	H_2 to O_2 Ratio
			Initial	Final					
88 g-U/L	1.71E+08	63.5	1.0	0.64	2972	1446	8.20E-02	3.99E-02	2.05
138 g-U/L	2.29E+08	116	1.0	0.63	1320	634	2.78E-02	1.34E-02	2.08
298 g-U/L	2.03E+08	262	1.0	0.58	1092	459	2.59E-02	1.09E-02	2.38

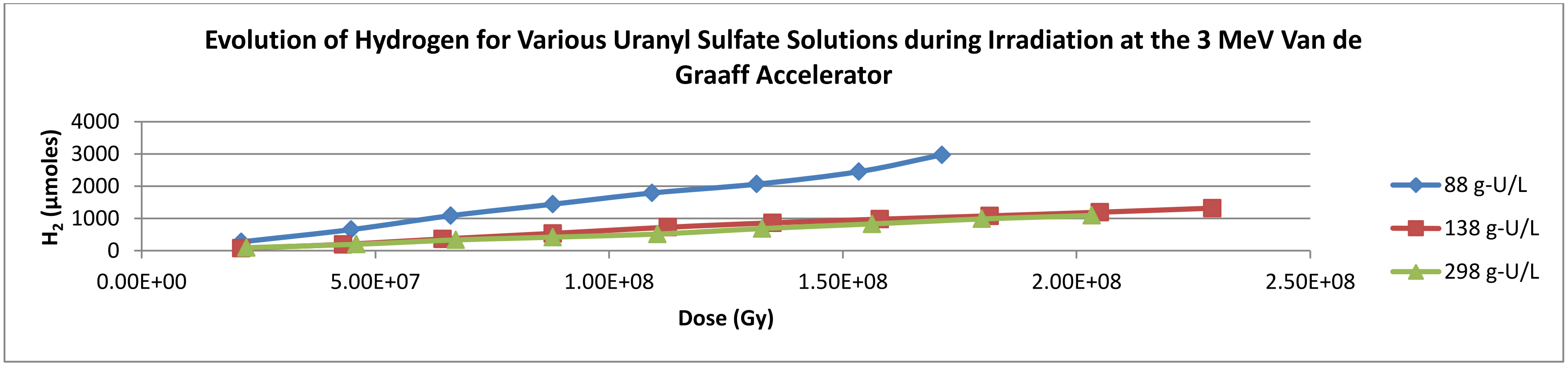

FIGURE 17 Hydrogen Evolution from UO_2SO_4 Solutions

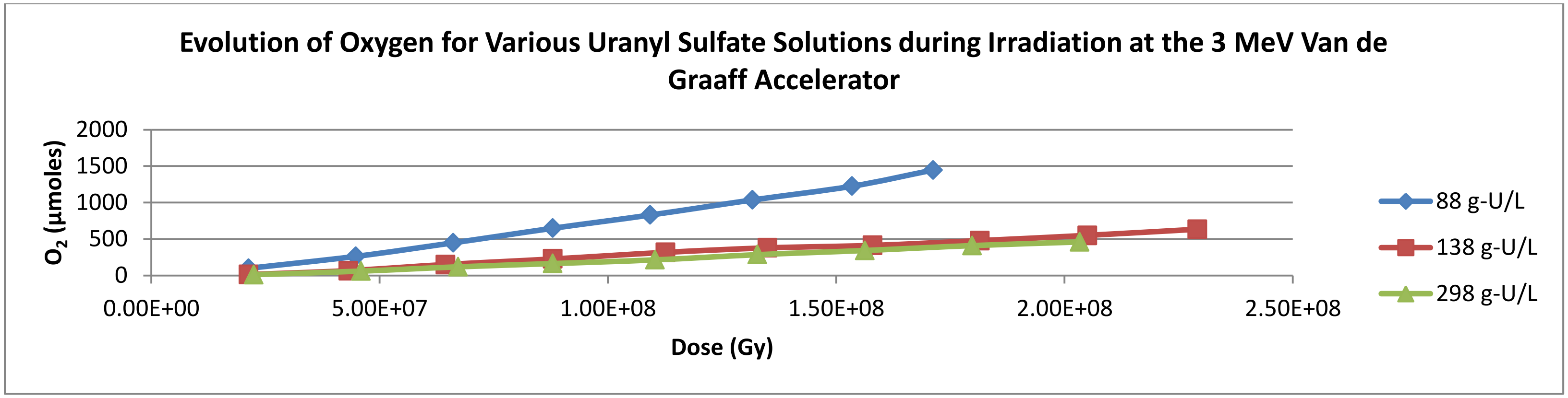

FIGURE 18 Oxygen Evolution from UO_2SO_4 Solutions

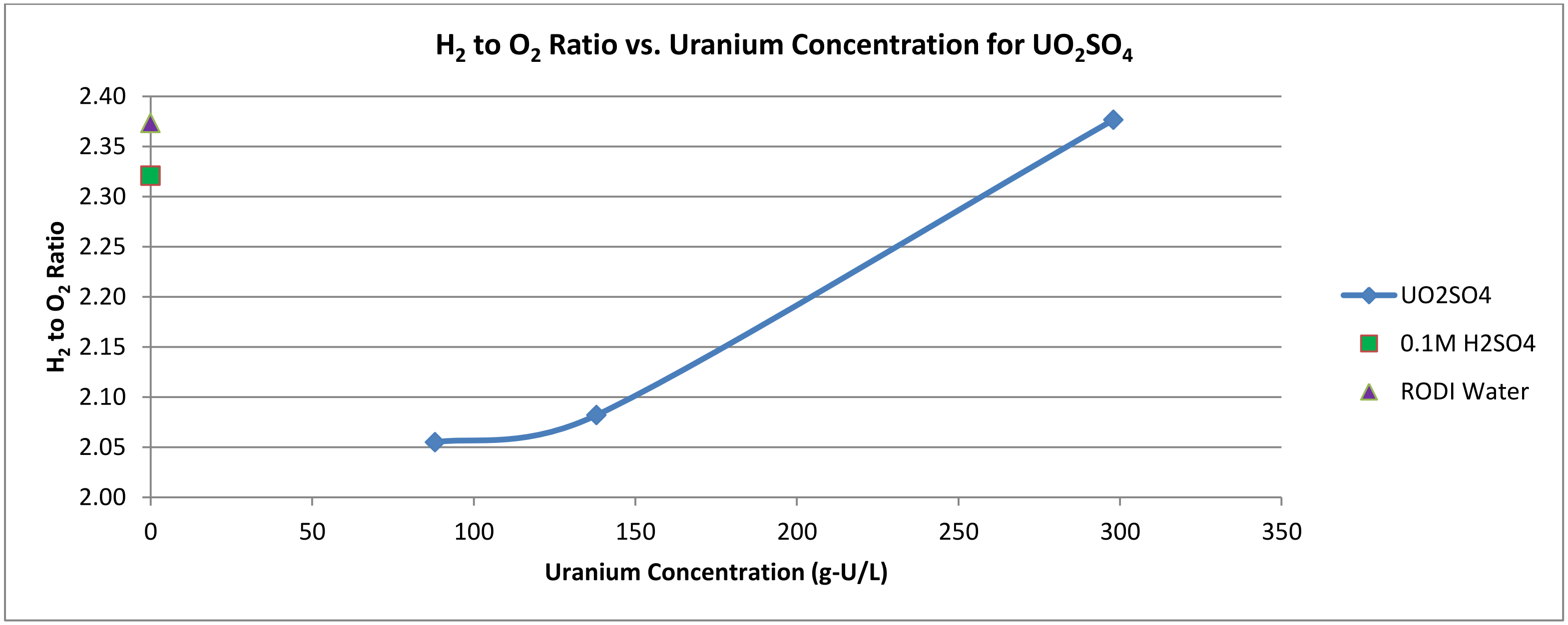

FIGURE 19 Hydrogen to Oxygen Ratio vs. UO_2SO_4 Concentration

10 CATALYTIC DESTRUCTION OF PEROXIDE IN URANYL SULFATE SOLUTIONS

Table 10 and Figures 20 and 21 provide experimental data for the irradiation of uranyl sulfate solutions either containing ferrous sulfate or in contact with zirconium metal. The figures show total µmoles of analyte (either hydrogen or oxygen) versus accumulated dose (Gy) during the 5-hr experiment. Each data point is at the sampling time for the analyte. Each graph displays the analyte versus dose for the various catalysts tested in uranyl sulfate solutions. These data follow with the tabular data such that the final point on the graph is the value listed in Table 10. Figure 22 presents the H/O ratios for the data. The following is a summary of that data.

From the result of the irradiation of uranyl sulfate solution, a method for destroying hydrogen peroxide (H_2O_2) as it forms in solution is needed. Initially, we tested zirconium metal pieces in solution with the thought that the reactor vessel itself could catalyze peroxide. This test failed, so we pursued the route of having an ion in solution so as to make intimate contact with molecules of H_2O_2 as they are produced during irradiation. The ferrous ion (Fe^{+2}) was chosen because it is known to react with H_2O_2 through the following equation.

$$Fe^{+2} + H_2O_2 \rightarrow Fe^{+3} + OH^- + OH\cdot$$

Because it acts as a catalyst, ferric ion is reduced back to ferrous. The results are discussed below.

10.1 PRECIPITATION OF URANYL PEROXIDE

The only solution that formed a precipitate was the solution with zirconium metal. Ferrous sulfate solutions were examined, but none of those solutions formed the uranyl-peroxide precipitate.

10.2 pH CHANGES

As with the uranyl sulfate solutions, without a catalyst added, the solution with zirconium metal showed a decrease in pH resulting from peroxide formation and precipitation. The solutions with ferrous sulfate added showed no change in pH.

10.3 HYDROGEN AND OXYGEN EVOLUTION

The sample with zirconium metal was similar in all respects to the sample without a catalyst. Hydrogen and oxygen production was high and the H_2 to O_2 ratio was greater than 2 (2.42:1). When ferrous sulfate was added as a catalyst, the total production of hydrogen and oxygen was significantly lower. Likewise, the ratio of hydrogen to oxygen was <2:1.

TABLE 10 Data from the Irradiation Uranyl Sulfate Solutions with Catalyst Added

Peroxide Catalyst	Energy Deposited (Gy)	Initial [$UO_2(SO_4)$] [g-U/L]	Final $UO_2(SO_4)$ [g-U/L]	pH		H_2 µmoles Total Produced	O_2 µmoles Total Produced	G-Value H_2/100 eV	G-Value O_2/100 eV	H_2 to O_2 Ratio
				Initial	Final					
9.94 mg/L $FeSO_4$	2.31E+08	123.5	No Precipitation	1.42	1.44	540	343	1.13E-02	7.16E-03	1.57
99.4 mg/L $FeSO_4$	2.20E+08	123.5	No Precipitation	1.42	1.37	462	302	9.80E-03	6.41E-03	1.53
Zr Metal	2.32E+08	298	260	1.0	0.67	1112	460	2.31E-02	9.55E-03	2.42

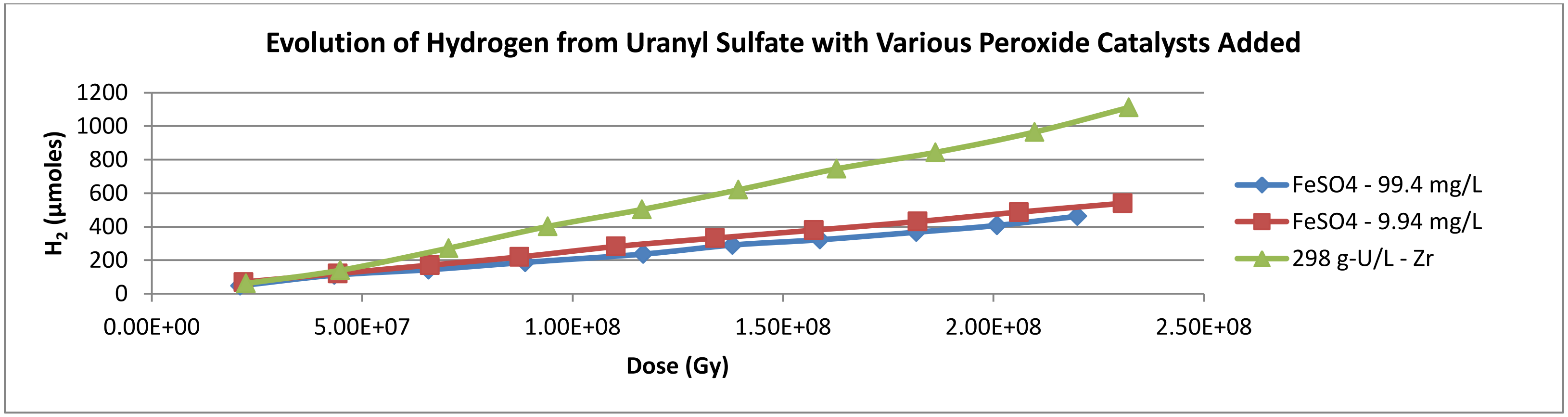

FIGURE 20 Hydrogen Evolution from UO_2SO_4 Solutions with Added Catalyst

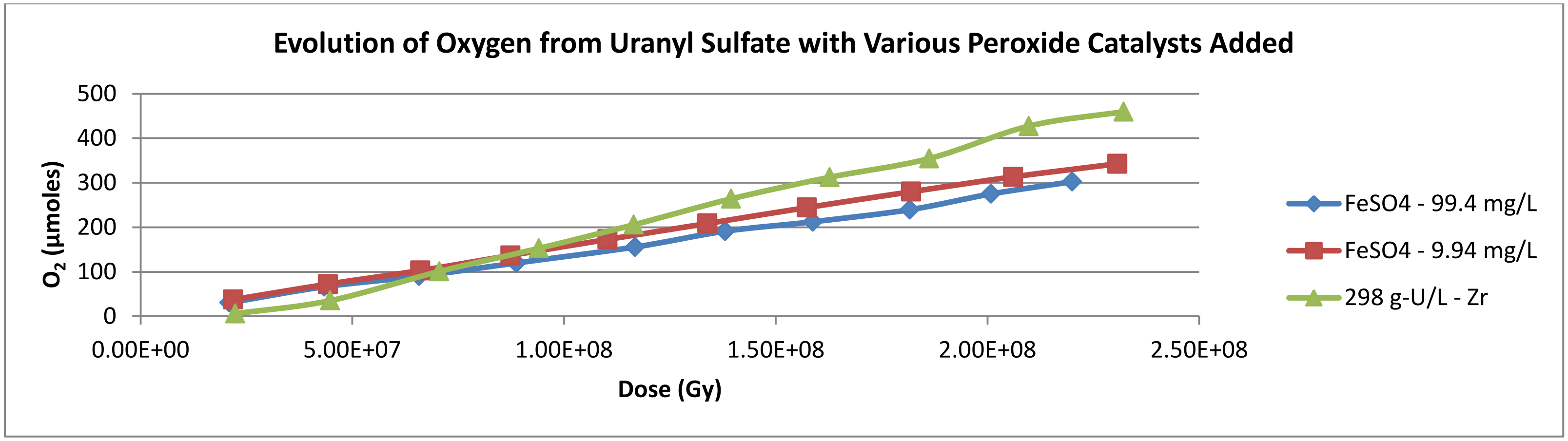

FIGURE 21 Oxygen Evolution from UO_2SO_4 Solutions with Added Catalyst

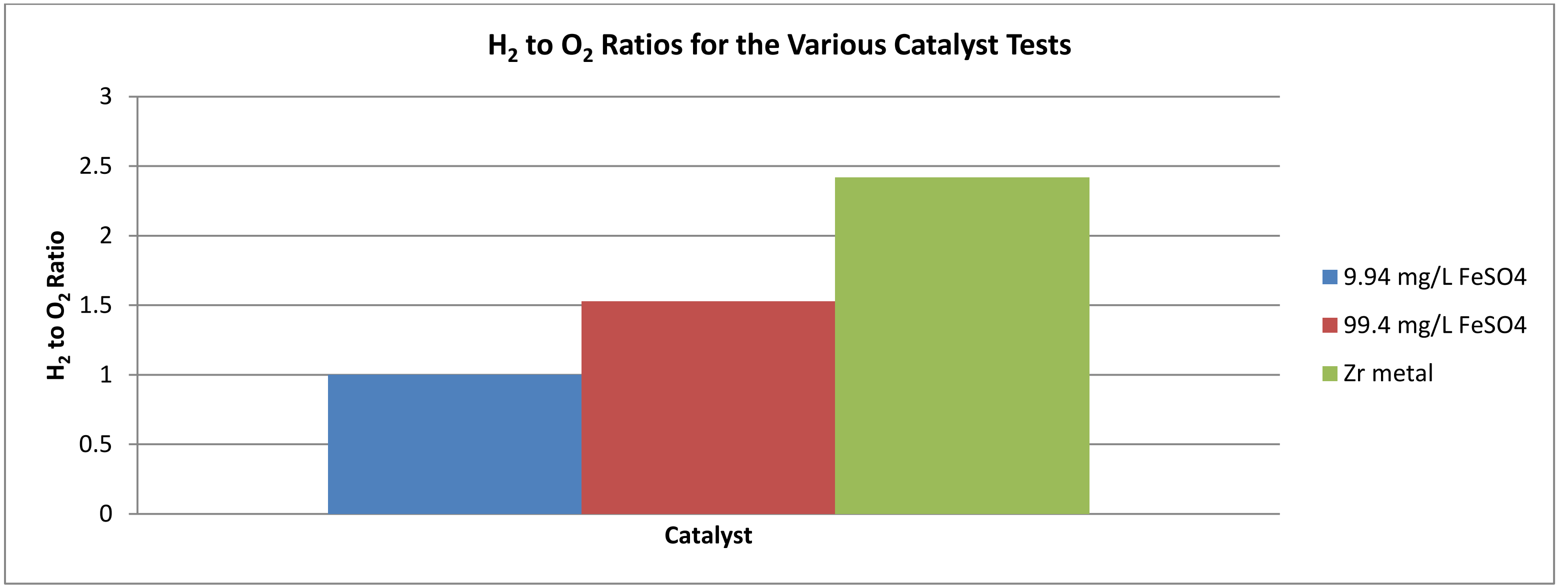

FIGURE 22 Hydrogen to Oxygen Ratio from UO_2SO_4 Solutions with Added Catalyst

Chemical Science and Engineering Division
Argonne National Laboratory
9700 South Cass Avenue, Bldg. 205
Argonne, IL 60439-4837

www.anl.gov

Argonne National Laboratory is a U.S. Department of Energy
laboratory managed by UChicago Argonne, LLC